Multielectron Reduction

DOI: 10.1002/anie.200701204

Electrochemical and Photochemical Behavior of a Ruthenium(II) Complex Bearing Two Redox Sites as a Model for the NAD^+/NADH Redox Couple**

*Hidenori Tannai, Take-aki Koizumi, Tohru Wada, and Koji Tanaka**

Multielectron reduction of small inorganic molecules such as CO_2, N_2, and H_2O to industrially valuable materials under mild conditions would enable the generation of sustainable natural resources.[1–3] The difficulty in reductive activation of those molecules is attributable to the undesirable formation of high-energy intermediates caused by one-electron transfer to the reaction centers. A few artificial light-driven multielectron-transfer systems have been constructed so far by using Ru-polypyridyl complexes as photosensitizers. Two electrons are stably stored on different electron-acceptor groups fixed in bridging ligands of trinuclear Ru_2-Ir and tetranuclear Ru_4 polypyridyl complexes under photoirradiation.[4] The groups of Rau and Sakai independently reported H_2 evolution in the photochemical reduction of H_2O catalyzed by binuclear Ru-Pd and Ru-Pt complexes, in which the Pt and Pd sites accept multielectrons and operate as the reaction centers.[5] MacDonnell and co-workers demonstrated the accumulation of up to four electrons in the bridging ligand of $[(phen)_2Ru(tatpq)Ru(phen)_2]^{4+}$ (phen = 1,10-phananthroline; tatpq = 9,11,20,22-tetraazatetrapyrido[3,2-a:2′3′-c:3″,2″-1:2‴,3‴]pentacene) under irradiation with visible light.[6] Recently, we showed that a mononuclear $[Ru^{II}(pbn)(bpy)_2]^{2+}$ (pbn = 2-pyridylbenzo[*b*]-1,5-naphthyridine; bpy = 2,2′-bipyridine), undergoes electrochemical and photochemical two-electron reduction in the presence of proton sources (Scheme 1)[7] and demonstrated the function of the resultant $[Ru(pbnH_2)(bpy)_2]^{2+}$ complex as a functional model of the nicotinamide adenine dinucleotide NAD^+/NADH redox couple that plays a key role as a reservoir/source of two electrons and one proton in various biological redox reactions. Along these lines, we have designed a new ruthenium(II) complex with a tridentate bbnp ligand (bbnp = 2,6-bis(benzo[*b*]-1,5-naphthyridin-6-yl)-4-*tert*-butylpyridine) with the intention to introduce the function of a reservoir/source of four electrons and four protons through a redox reaction.[8] Here we report the electro- and photochemical redox behavior of the mononuclear complex $[Ru(bbnp)(terpy)](PF_6)_2$ ($[\mathbf{1}](PF_6)_2$; terpy = 2,2′:6′,2″-terpyridine) and the corresponding two- and four-electron-reduced complexes $[Ru(bbnpH_2)(terpy)](PF_6)_2$ ($[\mathbf{1}H_2](PF_6)_2$) and $[Ru(bbnpH_4)(terpy)](PF_6)_2$ ($[\mathbf{1}H_4](PF_6)_2$).

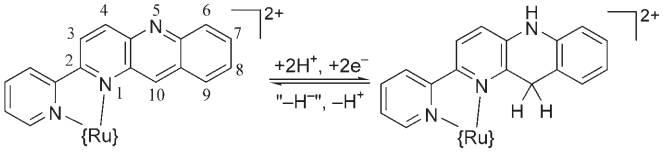

{Ru} = $[Ru(bpy)_2]$

Scheme 1. Reversible conversion between $[Ru(pbn)(bpy)_2]^{2+}$ and $[Ru(pbnH_2)(bpy)_2]^{2+}$ through a ligand-localized redox reaction.

The ruthenium(II) complex $[Ru(bbnp)(terpy)](PF_6)_2$ ($[\mathbf{1}](PF_6)_2$) was prepared by a two-step reaction. The chloride ligands of $[RuCl_3(terpy)]$ were not replaced by bbnp.[8] Thus, $[RuCl_3(bbnp)]$, obtained by the reaction of $RuCl_3 \cdot 3H_2O$ with bbnp, was treated with terpy in the presence of triethylamine to give the deep purple species $[Ru(bbnp)(terpy)]^{2+}$, which was isolated as the hexafluorophosphate salt (Scheme 2). The ESI-TOF mass spectrum of $[\mathbf{1}](PF_6)_2$ exhibited the parent peak at *m*/*z* 413 as a dication pattern. Treatment of $[\mathbf{1}](PF_6)_2$ with one and two equivalents of $Na_2S_2O_4$ in CH_3CN/H_2O (20:1 v/v) afforded $[Ru(bbnpH_2)(terpy)](PF_6)_2$ ($[\mathbf{1}H_2](PF_6)_2$) and $[Ru(bbnpH_4)(terpy)](PF_6)_2$ ($[\mathbf{1}H_4](PF_6)_2$), respectively. The parent peaks of $[\mathbf{1}H_2](PF_6)_2$ and $[\mathbf{1}H_4](PF_6)_2$ appeared at *m*/*z* 414 and 415, respectively, as dication patterns, indicating

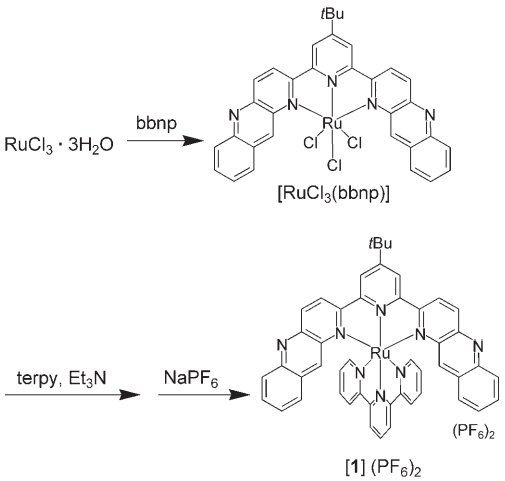

Scheme 2. Synthesis of $[Ru(bbnp)(terpy)](PF_6)_2$ ($[\mathbf{1}](PF_6)_2$).

[*] Dr. H. Tannai, Dr. T.-a. Koizumi, Dr. T. Wada, Prof. K. Tanaka
Coordination Chemistry Laboratories
Institute for Molecular Science
5–1, Higashiyama, Myodaiji
Okazaki, Aichi 444-8787 (Japan)
Fax: (+81) 564-59-5582
E-mail: ktanaka@ims.ac.jp

[**] This work was partly supported by a Grant-in-Aid for Scientific Research (A) (no. 18205009) from the Japan Society for the Promotion of Science.

Supporting information for this article is available on the WWW under http://www.angewandte.org or from the author.

increases in mass by two and four mass numbers relative to that of $[\mathbf{1}]^{2+}$ (m/z 413). The ^{1}H NMR spectra of $[\mathbf{1}H_2](PF_6)_2$ in $[D_6]$acetone displayed 22 different signals in the aromatic region, while that of $[\mathbf{1}H_4](PF_6)_2$ revealed 14 signals in the same region. The decrease in the symmetry of the molecular structure of $[\mathbf{1}H_2]^{2+}$ demonstrates the occurrence of the selective reduction of one of the benzo[*b*]-1,5-naphthyridin-6-yl groups (bnp) of the bbnp ligand with $2e^-$ and $2H^+$. The symmetry of the molecular structure of $[\mathbf{1}H_4]^{2+}$ reflects the reduction of the two bnp groups of the bbnp ligand of $[\mathbf{1}]^{2+}$ with $4e^-$ and $4H^+$. The NH protons of $[\mathbf{1}H_2]^{2+}$ and $[\mathbf{1}H_4]^{2+}$ were assigned to signals at $\delta = 8.45$ and 8.37 ppm, respectively, as those signals disappeared upon addition of D_2O to the solutions. The singlet peaks at $\delta = 3.45$ ppm for $[\mathbf{1}H_2]^{2+}$ and at $\delta = 3.28$ ppm for $[\mathbf{1}H_4]^{2+}$ with a total intensity of two and four protons, respectively, were assigned to the methylene groups at the 10-position of the reduced bnp groups.

The molecular structures of $[\mathbf{1}]^{2+}$ and $[\mathbf{1}H_4]^{2+}$ were determined by X-ray crystallographic analyses.[9] The parent complex $[\mathbf{1}]^{2+}$ displays a distorted octahedral configuration formed by central three nitrogen atoms of bbnp and three nitrogen centers of terpy (Figure 1). The Ru–N bond lengths to bbnp were slightly longer (≈ 0.5 Å) than those to terpy, which were comparable to those in $[Ru(terpy)_2]^{2+}$.[10] This may be ascribed to steric repulsion between the two external bnp groups and an internal terpy ligand. The crystallographically imposed twofold rotation axis at the center of $[\mathbf{1}H_4]^{2+}$ manifests the disorder of the *tert*-butyl group of the bbnpH_4 ligand over two positions. The Ru–N bond lengths for $[\mathbf{1}H_4]^{2+}$ are not significantly different from those of $[\mathbf{1}]^{2+}$, but the C1–C2 and C2–C3 bond lengths for $[\mathbf{1}H_4]^{2+}$ (1.501(8) and 1.510(7) Å, respectively) are clearly longer than those for $[\mathbf{1}]^{2+}$ (1.388(6)–1.399(6) Å) and the other C–C bonds of the aromatic rings of bbnpH_4 in $[\mathbf{1}H_4]^{2+}$ (1.35(1)–1.419(7) Å). The lengths of the C1–C2 and C2–C3 bonds of $[\mathbf{1}H_4]^{2+}$ correspond to single bonds rather than aromatic C=C bonds. These results also confirm the protonation on the nitrogen atom at the 5-position and the hydrogenation of the carbon atom at the 10-position of the bnp groups in the four-electron reduction of $[\mathbf{1}]^{2+}$ in aqueous conditions.

The cyclic voltammogram (CV) of $[\mathbf{1}](PF_6)_2$ exhibited four reversible redox couples at $E_{1/2} = +1.48$, -0.62, -0.88, and -1.42 V (vs. SCE) in CH_3CN. The redox reactions at $E_{1/2} = +1.48$ V and -1.42 V are tentatively associated with the metal-centered Ru^{II}/Ru^{III} couple and the ligand-localized (terpy$^{-\bullet}$/terpy) couple, based on the redox behavior of $[Ru(terpy)_2]^{2+}$.[11] The remaining redox reactions at $E_{1/2} = -0.62$ and -0.88 V result from the two successive ligand-localized (bnp,bnp)/(bnp$^{-\bullet}$,bnp) and (bnp$^{-\bullet}$,bnp)/(bnp$^{-\bullet}$,bnp$^{-\bullet}$) couples. On the other hand, an irreversible anodic wave emerged at $E_{pa} = +1.11$ V in the CV of $[\mathbf{1}H_2](PF_6)_2$ owing to the oxidation of the bnpH_2 group. The reversible (bnp/bnp$^{-\bullet}$) and Ru^{II}/Ru^{III} redox couples were observed at $E_{1/2} = -0.74$ V and $+1.69$ V in CH_3CN, respectively. The bnp/bnp$^{-\bullet}$ redox couple completely disappeared in the CV of $[\mathbf{1}H_4](PF_6)_2$, which displayed an irreversible oxidation wave at $E_{pa} = +1.14$ V and a metal-centered reversible Ru^{II}/Ru^{III} couple at $E_{1/2} = +1.68$ V. In contrast to the CV measured in CH_3CN, in H_2O/CH_3CN (7:3 v/v, pH 7.92) $[\mathbf{1}]^{2+}$ exhibits one irreversible cathodic wave at $E_{pc} = -0.58$ V and the corresponding anodic wave at $E_{pa} = +0.58$ V (Figure 2). The potentiostatic electrolysis of $[\mathbf{1}](PF_6)_2$ at -0.69 V consumed four electrons per molecule (4 F/mol; F = Faraday), and the complete conversion from $[\mathbf{1}]^{2+}$ to $[\mathbf{1}H_4]^{2+}$ was confirmed by the ESI-TOF mass spectrum of the reduction product. Furthermore, oxidation of $[\mathbf{1}H_4]^{2+}$ at $+0.77$ V smoothly regenerated $[\mathbf{1}]^{2+}$ [Eq. (1)].

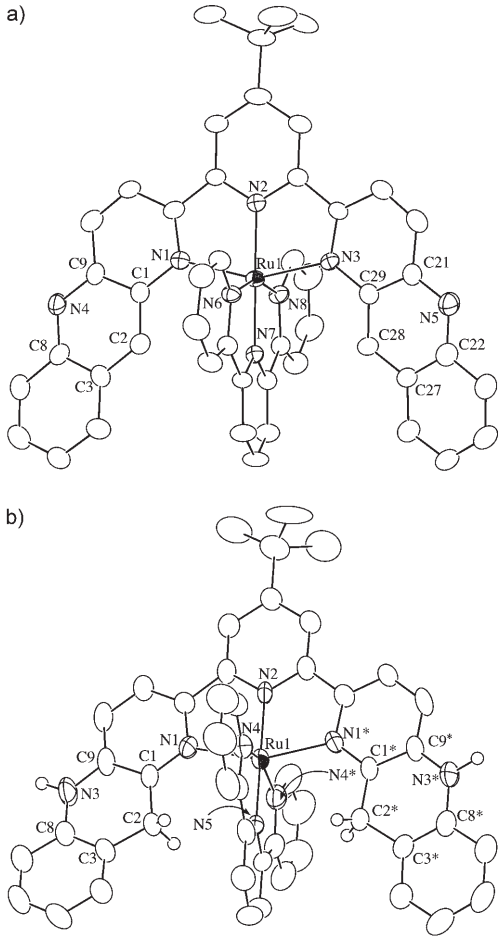

Figure 1. ORTEP drawing of a) $[\mathbf{1}]^{2+}$ and b) $[\mathbf{1}H_4]^{2+}$. Thermal ellipsoids are drawn at the 50% probability level. Hydrogen atoms except for those at C2, C2*, N3, and N3* in $[\mathbf{1}H_4]^{2+}$ are omitted for clarity. One position of a disordered *tert*-butyl group in $[\mathbf{1}H_4]^{2+}$ is shown. Symmetry code: *, $-x+1$, y, $-z+3/2$.

The UV/Vis absorption spectrum of $[\mathbf{1}](PF_6)_2$ gradually changed to that of $[\mathbf{1}H_4](PF_6)_2$ in CH_3CN/TEOA (4:1 v/v, TEOA = triethanolamine) under illumination with a Xe lamp (Figure 3a). During the initial photochemical reaction of $[\mathbf{1}]^{2+}$, a new band appeared at $\lambda_{max} = 974$ nm owing to the formation of $[\mathbf{1}]^{+}$; the electrolysis of $[\mathbf{1}]^{2+}$ at -0.75 V and -1.07 V in CH_3CN generates $[\mathbf{1}]^{+}$ and $[\mathbf{1}]^{0}$, which develop absorption bands in the near-infrared (NIR) region at $\lambda_{max} =$ 972 nm and 1014 nm, respectively (Figure 3b). The intensity of the band at 974 nm then gradually decreased with time, while a band at 427 nm corresponding to $[\mathbf{1}H_4]^{2+}$ appeared and increased in intensity with time. Similarly, the photochemical reduction of $[\mathbf{1}H_2]^{2+}$ to $[\mathbf{1}H_4]^{2+}$ conducted under

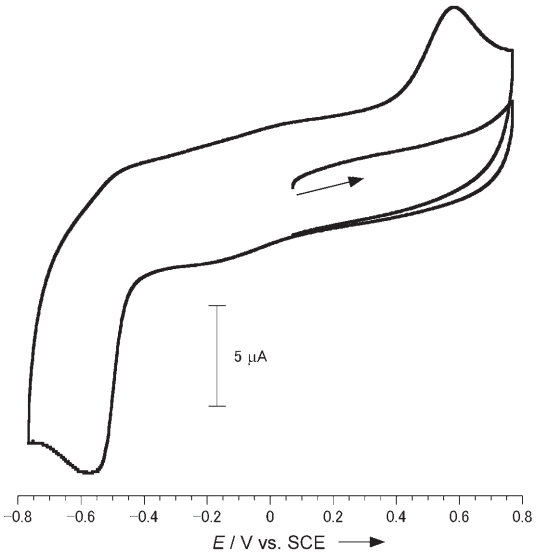

Figure 2. Cyclic voltammogram of $[\mathbf{1}](PF_6)_2$ in H_2O/CH_3CN (7:3 v/v) at pH 7.92 (SCE = saturated calomel electrode). The arrow denotes the scan direction.

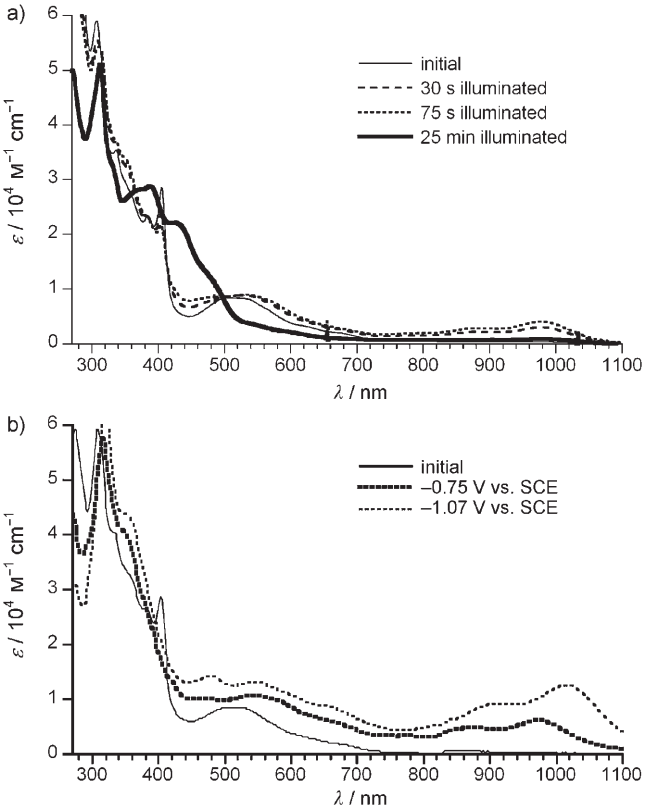

Figure 3. a) Changes in the UV/Vis/NIR absorption spectra of $[\mathbf{1}](PF_6)_2$ in CH_3CN/TEOA (4:1 v/v) under illumination with a Xe lamp. b) Spectroelectrochemical measurements of $[\mathbf{1}](PF_6)_2$ in CH_3CN solution.

similar conditions also transiently displayed a band for $[\mathbf{1}H_2]^+$ at $\lambda_{max} = 978$ nm at the beginning of the reaction.

Note that the addition of one equivalent of *p*-toluenesulfonic acid to $[\mathbf{1}]^+$ generated by the electrolysis of $[\mathbf{1}]^{2+}$ in CH_3CN caused disproportionation of the protonated species $[\mathbf{1}]^+$ to produce a 1:1 mixture of $[\mathbf{1}]^{2+}$ and $[\mathbf{1}H_2]^{2+}$ in solution. We have shown that the excited state of the analogous $[Ru^{II}(pbn)(bpy)_2]^{2+}$ species ($\tau = 140$ ns in CH_3CN) is reductively quenched by TEOA to give $[Ru^{II}(pbn^{-\bullet})(bpy)_2]^+$, protonation of which is very fast in water.[7b] The present photochemical four-electron reduction of $[\mathbf{1}]^{2+}$, therefore, is reasonably explained by the reactions shown in Equations (2) and (3).

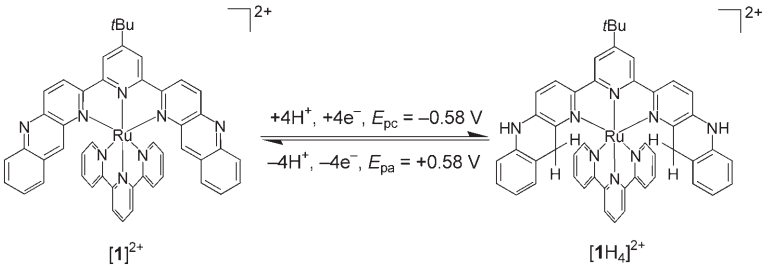

(1)

$$[\mathbf{1}]^{2+} * \xrightarrow{\text{TEOA}} [\mathbf{1}]^{+} \xrightarrow{H^+} [\mathbf{1}H]^{2+} \rightarrow 1/2[\mathbf{1}]^{2+} + 1/2[\mathbf{1}H_2]^{2+} \quad (2)$$

$$[\mathbf{1}H_2]^{2+} * \xrightarrow{\text{TEOA}} [\mathbf{1}H_2]^{+} \xrightarrow{H^+} [\mathbf{1}H_3]^{2+} \rightarrow 1/2[\mathbf{1}H_2]^{2+} + 1/2[\mathbf{1}H_4]^{2+} \quad (3)$$

Reductive quenching of the photochemically excited $[\mathbf{1}]^{2+}*$ by TEOA produces $[\mathbf{1}]^+$. Protonation of $[\mathbf{1}]^+$ under the experimental conditions and subsequent disproportionation of the resultant $[\mathbf{1}H]^{2+}$ affords a 1:1 mixture of $[\mathbf{1}]^{2+}$ and $[\mathbf{1}H_2]^{2+}$ [Eq. (2)]. The mechanism for the photochemical reduction of $[\mathbf{1}]^{2+}$ to $[\mathbf{1}H_2]^{2+}$ [Eq. (2)] is essentially the same as that of $[Ru^{II}(pbn)(bpy)_2]^{2+}$ affording $[Ru^{II}(pbnH_2)(bpy)_2]^{2+}$ with a quantum yield of 0.21 under irradiation at 355 nm in CH_3CN/TEOA.[7b] Further photoirradiation of $[\mathbf{1}H_2]^{2+}$ in the presence of TEOA results in the formation of $[\mathbf{1}H_2]^+$, protonation of which, followed by disproportionation, will generate $[\mathbf{1}H_2]^{2+}$ and $[\mathbf{1}H_4]^{2+}$ [Eq. (3)]. Two photons are required to complete the reduction from $[\mathbf{1}]^{2+}$ to $[\mathbf{1}H_2]^{2+}$, and from $[\mathbf{1}H_2]^{2+}$ to $[\mathbf{1}H_4]^{2+}$. On the other hand, $[\mathbf{1}]^{2+}$ is continuously reduced to $[\mathbf{1}H_4]^{2+}$ through $[\mathbf{1}H_2]^{2+}$. So, photochemical reduction as shown in Equation (3) was conducted independently by using $[\mathbf{1}H_2]^{2+}$ under illumination with visible light (532 nm), and the quantum yield of the reaction was determined as 0.38. Thus, the electrochemical and photochemical reduction of $[\mathbf{1}]^{2+}$ efficiently accumulates four electrons through the formation of two C−H and two N−H bonds in the bbnp ligand.

In conclusion, a ruthenium(II) complex bearing bbnp redox sites aiming for the function of the NAD^+/NADH redox couple was prepared and characterized. The bbnp ligand of $[\mathbf{1}]^{2+}$ undergoes two successive one-electron-reduction processes in aprotic media, while it undergoes four-electron reduction in aqueous solutions as a result of participation of four protons in the redox reaction. We

successfully isolated two-electron- and four-electron-reduced forms of $[\mathbf{1}]^{2+}$ in the reaction of $[\mathbf{1}]^{2+}$ with one and two equivalents of $Na_2S_2O_4$ under aqueous conditions. The four-electron reduction of the monomeric $[\mathbf{1}]^{2+}$ through the repetition of one-electron reduction, protonation of the reduced form, and subsequent disproportionation of the protonated species could provide new methodologies for electrochemical and photochemical multielectron reductions catalyzed by metal complexes.

Experimental Section

See the Supporting Information for experimental details including synthetic procedures, physical measurements, X-ray diffraction studies, UV/Vis absorption spectra of $[\mathbf{1}](PF_6)_2$, $[\mathbf{1}H_2](PF_6)_2$, and $[\mathbf{1}H_4](PF_6)_2$ (Figure S1), cyclic voltammograms of $[\mathbf{1}](PF_6)_2$, $[\mathbf{1}H_2](PF_6)_2$, and $[\mathbf{1}H_4](PF_6)_2$ in CH_3CN (Figure S2), changes in absorption spectra during the course of photoreduction of $[\mathbf{1}](PF_6)_2$ and $[\mathbf{1}H_2](PF_6)_2$ (Figures S3 and S4, respectively), and selected bond lengths and angles of $[\mathbf{1}](PF_6)_2{\cdot}0.5C_2H_5OC_2H_5$ and $[\mathbf{1}H_4](PF_6)_2{\cdot}CH_3CN{\cdot}C_2H_5OC_2H_5$ (Tables S1 and S2, respectively).

Received: March 19, 2007
Revised: May 30, 2007
Published online: August 7, 2007

Keywords: NADH model · photoreduction · protonation · redox chemistry · ruthenium

[1] a) H. Arakawa et al., *Chem. Rev.* **2001**, *101*, 953 – 996 (see Supporting Information); b) K. Tanaka, D. Ooyama, *Coord. Chem. Rev.* **2002**, *226*, 211 – 218; c) E. Fujita, *Coord. Chem. Rev.* **1999**, *185–186*, 373 – 384; d) J. Mascetti, F. Galan, I. Pàpai, *Coord. Chem. Rev.* **1999**, *190–192*, 557 – 576.

[2] a) R. R. Schrock, *Acc. Chem. Res.* **2005**, *38*, 955 – 962; b) F. Barrière, *Coord. Chem. Rev.* **2003**, *236*, 71 – 89.

[3] a) A. F. Heyduk, D. G. Nocera, *Science* **2001**, *293*, 1639 – 1641; b) M. Grätzel, *Acc. Chem. Res.* **1981**, *14*, 376 – 384.

[4] a) S. M. Molnar, G. Nallas, J. S. Bridgewater, K. J. Brewer, *J. Am. Chem. Soc.* **1994**, *116*, 5208 – 5209; b) M. M. Ali, H. Sato, M. Haga, K. Tanaka, A. Yoshimura, T. Ohno, *Inorg. Chem.* **1998**, *37*, 6176 – 6180.

[5] a) S. Rau, B. Schäfer, D. Gleich, E. Anders, M. Rudolph, M. Friedrich, H. Görls, W. Henry, J. G. Vos, *Angew. Chem.* **2006**, *118*, 6361 – 6364; *Angew. Chem. Int. Ed.* **2006**, *45*, 6215 – 6218; b) H. Ozawa, M. Haga, K. Sakai, *J. Am. Chem. Soc.* **2006**, *128*, 4926 – 4927.

[6] a) R. Konduri, H. Ye, F. M. MacDonnell, S. Serroni, S. Campagna, K. Rajeshwar, *Angew. Chem.* **2002**, *114*, 3317 – 3319; *Angew. Chem. Int. Ed.* **2002**, *41*, 3185 – 3187; b) R. Konduri, N. R. de Tacconi, K. Rajeshwar, F. M. MacDonnell, *J. Am. Chem. Soc.* **2004**, *126*, 11621 – 11629; c) N. R. de Tacconi, R. O. Lezna, R. Konduri, F. Ongeri, K. Rajeshwar, F. M. MacDonnell, *Chem. Eur. J.* **2005**, *11*, 4327 – 4339.

[7] a) T. Koizumi, K. Tanaka, *Angew. Chem.* **2005**, *117*, 6041 – 6044; *Angew. Chem. Int. Ed.* **2005**, *44*, 5891 – 5894; b) D. Polyansky, D. Cabelli, J. T. Muckerman, E. Fujita, T. Koizumi, T. Fukushima, T. Wada, K. Tanaka, *Angew. Chem.* **2007**, *119*, 4247 – 4250; *Angew. Chem. Int. Ed.* **2007**, *46*, 4169 – 4172.

[8] H. Tannai, T. Koizumi, K. Tanaka, *Inorg. Chim. Acta* **2007**, *360*, 3075 – 3082.

[9] CCDC-638606 ($[\mathbf{1}]^{2+}$) and CCDC-638607 ($[\mathbf{1}H_4]^{2+}$) contain the supplementary crystallographic data for this paper. These data can be obtained free of charge from The Cambridge Crystallographic Data Centre via www.ccdc.cam.ac.uk/data_request/cif.

[10] K. Lashgari, M. Kritikos, R. Norrestam, T. Norrby, *Acta Crystallogr. Sect. C* **1999**, *55*, 64 – 67.

[11] T. Koizumi, K. Tanaka, *Inorg. Chim. Acta* **2005**, *358*, 1999 – 2004.

